PERGAMON

International Journal of Heat and Mass Transfer 45 (2002) 3715–3724

International Journal of HEAT and MASS TRANSFER

www.elsevier.com/locate/ijhmt

Single-sided steam condensing inside a rectangular horizontal channel

W. Yu [a,*], S.U.-S. Choi [a], D.M. France [b,1], M.W. Wambsganss [a]

[a] *Energy Technology Division, Argonne National Laboratory, 9700 S. Cass Avenue, Building 335, Argonne, IL 60439, USA*
[b] *Department of Mechanical Engineering, M/C 251, University of Illinois at Chicago, 842 W. Taylor Street, Chicago, IL 60607-7022, USA*

Received 2 January 2002; received in revised form 16 February 2002

Abstract

Heat transfer rates for steam condensation were experimentally studied in a horizontal channel with: bottom-sided cooling only, relatively small vertical channel height of 3.137 mm, width of 18.898 mm, and cooled length of 3 m. Experiments were performed at low mass flux (20–50 kg/m^2 s) and at pressures of 170–620 kPa applicable to large drum-type heat exchangers. Results for this rather unique combination of parameters were compared to: (1) trends from other better established condensing systems, and (2) the few available condensing correlations that cover most of the parameter ranges of these experiments. Modifications are presented which better predict the data.

1. Introduction

Forced convective condensation inside horizontal channels appears in a variety of applications and in such industries as electric utilities, chemical processing, refrigeration and air-conditioning. Over the last several decades, many analytical and experimental studies on condensation heat transfer inside horizontal channels have been reported in the engineering literature (see [1] for a recent review). Most of these studies have focused on condensation inside horizontal circular tubes cooled around the entire circumference. There are, however, applications in which the condensation occurs only over a partial circumference. One such application is in cylindrical paper dryers where steam condensation occurs inside of large diameter (1–2 m) cylinders (drums). A typical paper production machine includes dozens of these dryers. A recent innovation in the design, Choi et al. [2], has the condensation occurring inside of small rectangular channels at the inside cylinder surface. For this application of one-sided condensation in small horizontal rectangular channels, little research work is available. Lu and Suryanarayana [3] addressed this geometry, but no predictive results were included for single-sided condensation. The present study focused on obtaining and understanding data, and predictive equations for condensation heat transfer in this configuration.

2. Test apparatus and procedure

In order to measure condensing heat transfer rates in small horizontal channels cooled on one side, a test facility was designed and fabricated as shown schematically in Fig. 1. The facility consists of four closed flow systems (loops) as shown in Fig. 1 and is capable of operating at pressures up to 1035 kPa and temperatures up to 180 ° C.

The test section consists of a horizontal rectangular channel cooled from below and insulated on the three remaining surfaces. The working fluid is supplied to the test section as superheated vapor from the water/steam

* Corresponding author. Tel.: +1-630-252-6153; fax: +1-630-252-5568.

E-mail addresses: wyu@anl.gov (W. Yu), choi@anl.gov (S.U.-S. Choi), dfrance@uic.edu (D.M. France), wambsganss@anl.gov (M.W. Wambsganss).

[1] Tel.: +1-312-996-0520; fax: +1-312-996-8664.

0017-9310/02/$ - see front matter
PII: S0017-9310(02)00087-X

Nomenclature

A	area
C_p	specific heat
D	diameter
f	function symbol
G	mass flux
h	heat transfer coefficient
H	height
i	enthalpy
i_{fg}	latent heat
L	length
$\dot{m}$	mass flow rate
Nu	Nusselt number
p	pressure
Pr	Prandtl number of liquid
q	heat transfer rate
Re	Reynolds number
T	temperature
W	width
x	quality
z	axial location

Greek symbols

δ	thickness
Δ	differential
μ	viscosity
ρ	density

Subscripts

amb	ambient
c	coolant
env	environment
h	hydraulic
in	inlet
L	liquid
out	outlet
r	reduced
s	steam
V	vapor
w	wall

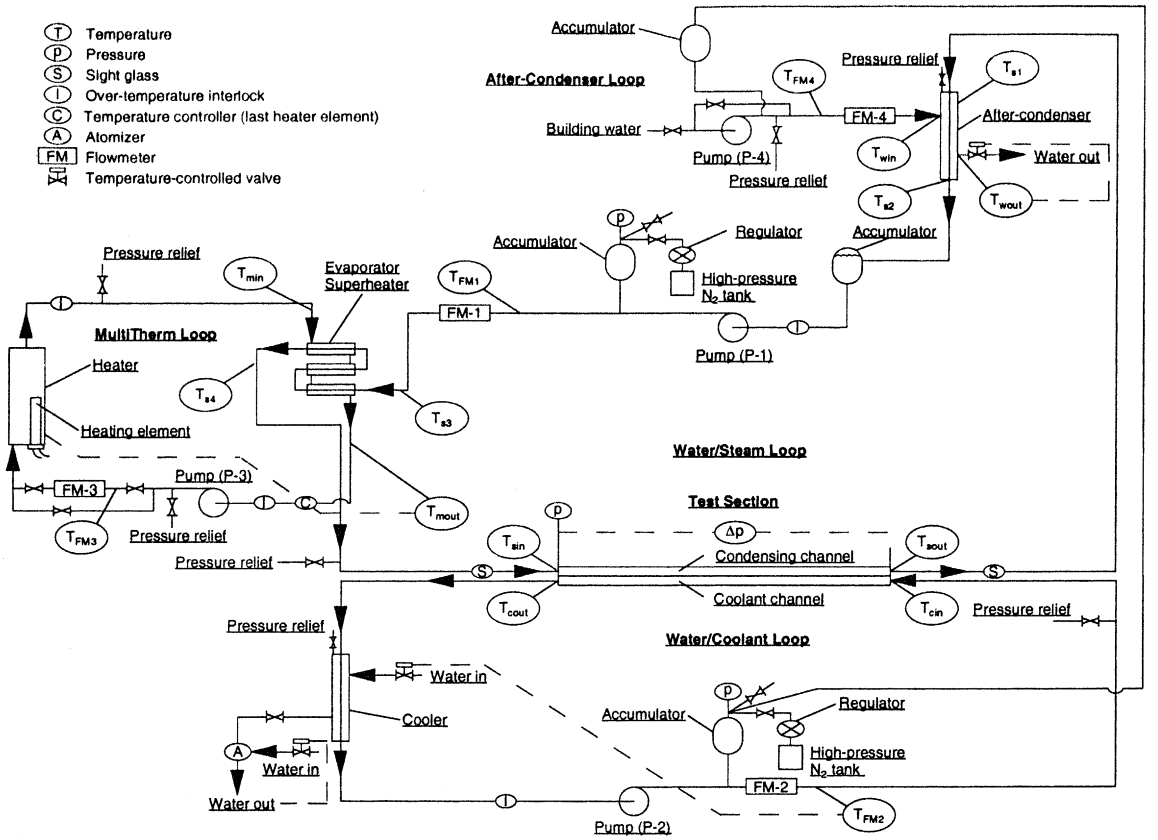

Fig. 1. Schematic representation of condensing heat transfer test apparatus.

loop, and liquid water is circulated in the water/coolant loop to cause condensation of the working fluid. The MultiTherm loop supplies heat to superheat the working fluid at the test section inlet, and the after-condenser loop supplies coolant to produce subcooled liquid water downstream of the test section.

2.1. Water/steam loop

Water is the working fluid for the experiments, and it is contained in the water/steam loop. As shown in Fig. 1, Pump P-1 is used to pump water in the liquid state from the after-condenser into the evaporator/superheater. A rotameter is used to measure the volumetric flow. Adding a temperature measurement at the flowmeter allows calculation of the water density at the flowmeter and the mass flow rate. The water flow rate was accurately controlled using an AC adjustable-frequency drive.

In the evaporator/superheater heat exchanger, the working fluid is boiled and heated to a superheated vapor for introduction to the test section. The superheated inlet is important for two reasons. It allows the accurate determination of the thermodynamic properties of the fluid, and it precludes any preferential flow distribution that can exist with a two-phase inlet transitioning from the flow circuit duct (with associated bends) to the test section.

Heat is supplied, to boil the working fluid in the evaporator/superheater, from a flowing high temperature liquid (MultiTherm). Using this high temperature liquid allows the complete boiling of the working fluid from subcooled liquid to superheated vapor while eliminating critical heat flux problems. The evaporator/superheater heat exchanger is a shell-and-tube counterflow design; it was designed specifically for this boiling-water/MultiTherm application.

In the water/steam loop, the water pressure at the test section inlet is controlled with the accumulator and high-pressure nitrogen tank shown in Fig. 1.

2.2. MultiTherm loop

The MultiTherm loop supplies liquid MultiTherm up to 230 °C to the evaporator/superheater to produce superheated steam for the test section. Seven electrical resistance cartridge heaters are used to supply heat to the MultiTherm as shown in Fig. 1. The heater sizes are varied such that any power input can be maintained up to a maximum of 15 kW.

As shown in Fig. 1, the MultiTherm liquid is pumped by Pump P-3 from the evaporator/superheater to the heater. A piston-type flowmeter (MAX Machinery) is used to measure the volumetric flow. A temperature sensor just upstream from the flowmeter provides a measure of the liquid temperature, which, in turn, allows calculation of the MultiTherm liquid density at the flowmeter and the mass flow rate. The heat that is transferred to the steam is controlled by (1) the MultiTherm flow rate, which is controlled to a desired value by an AC adjustable-frequency drive, and (2) the heater power.

2.3. Water/coolant loop

The water/coolant loop provides cool liquid water to condense the working fluid water in the test section. Laboratory water is used in the cooler heat exchanger to subcool the coolant water from the test section. Pump P-2 moves water from the cooler into the coolant channel. A turbine-type flowmeter (Flowdata) is used to measure the volumetric flow. A temperature sensor just downstream from the flowmeter provides a measure of the water temperature, which, in turn, allows calculation of the water density at the flowmeter and the mass flow rate. The volumetric flow can be controlled to a desired value with an AC adjustable-frequency drive.

The pressure of the water/coolant loop is set by the nitrogen supply and accumulator shown in Fig. 1. The pressure was kept high enough to prevent boiling of the coolant in all tests.

2.4. After-condenser loop

The after-condenser loop provides cool liquid laboratory water to reject heat from the working fluid exiting the test section to bring it to the subcooled liquid state. This condition is necessary prior to pumping, and the heat transfer occurs in the after-condenser heat exchanger. The laboratory water is pressurized with Pump P-4, and an accumulator is used to avoid its boiling. The laboratory water flow rate is controlled by varying the pump speed, and a turbine-type flowmeter (Flowdata) is used to measure the flow rate. This system sets the water temperature at the inlet to the evaporator/superheater.

2.5. Test section

The test section, shown schematically in Fig. 2, consists of two, horizontal, rectangular channels mounted one above the other. The steam flows in the top (condensing) test channel with the coolant flowing countercurrent in the bottom (coolant) channel. The condensing channel is 18.898 mm wide and 3.137 mm high with a condensing length of 3 m. This configuration of one-sided condensing on the bottom of the horizontal channel puts the condensate film between the steam and the cool surface as encountered in one-sided condensing applications discussed previously.

The two horizontal channels comprising the test section are made of aluminum and were welded continuously over their mating surfaces. This process minimized

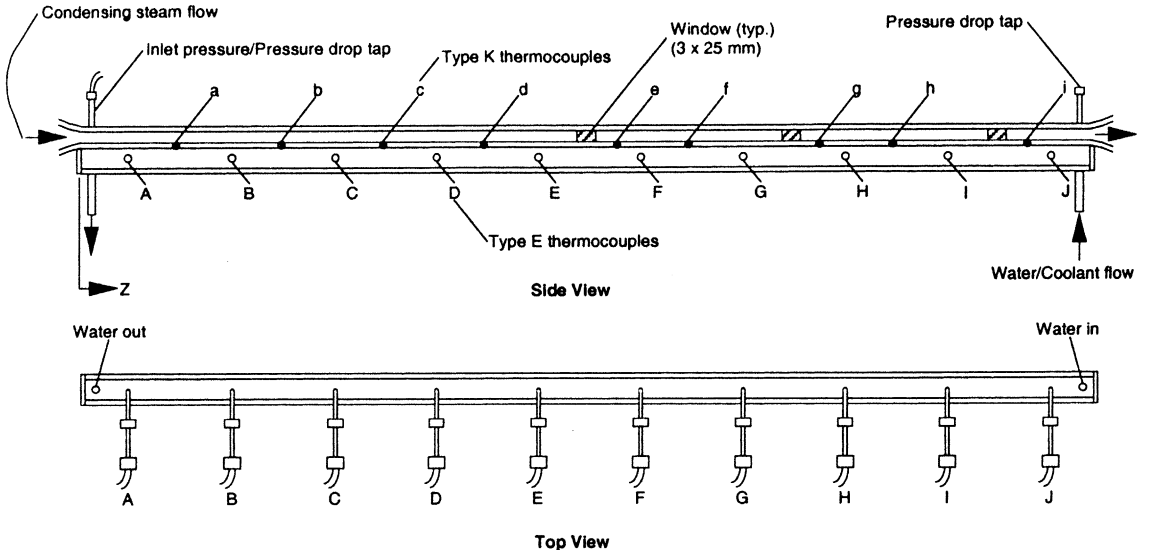

Fig. 2. More detailed schematic representation of test section.

thermal resistance between the two channels. Nine Type K thermocouples (lettered a–i in Fig. 2) were positioned in the wall between the condensing and the coolant channels; they divide the test section into segments, each 0.305 m in length. The local bulk coolant temperatures, used to calculate the local heat flux in the test section, were measured with Type E thermocouples at 10 axial locations and are lettered A–J in Fig. 2. These stream coolant thermocouples are positioned axially between wall thermocouples so that their intrusions into the flow have minimal effect on the wall temperature readings. The inlet and outlet temperatures of both the condensing and coolant channels were also measured with Type E sheathed thermocouples located in the fluid streams.

Inlet steam pressure and overall pressure drop across the condensing channel were measured during experimentation. The pressure at the condensing channel inlet was measured with a piezoelectric pressure transducer (Endevco), while the overall condensing channel pressure drop was measured with a variable-reluctance differential pressure transducer (Validyne). The overall pressure drop, together with the pressure and temperature at the condensing channel inlet, provided a means to calculate the distribution of the steam temperature along the condensing channel.

The test section was well insulated thermally to minimize heat loss to the environment. However, it was not negligible, and heat loss tests were conducted to quantify this loss as discussed subsequently.

Water entered the test section slightly superheated so that its state could be determined easily and accurately. Then heat loss at the inlet end of the test section caused a small amount of steam condensation so that the steam was slightly into the quality region as it encountered the coolant channel. Water exited the test section as a two-phase flow or as subcooled liquid. Subsequently it was subcooled in the after-condenser to a level required for pumping.

3. Data acquisition and reduction

A data acquisition system (DAS), consisting of a PC (Gateway 2000) and multiplexor (Hewlett-Packard, Model HP75000), was assembled to record data. A data acquisition code was written in Hewlett-Packard Instrument Basic to control all measurements. The code includes all calibration equations and conversions to engineering units. The DAS provides an on-screen display of the outputs of all sensors converted to engineering units. It also provides time charts of representative in-stream and wall-temperature measurements used for steady state determination. Once test conditions were achieved, all sensor-output voltages were read 30 times by the DAS and averaged in three sets of 10 readings each. As a check on steady state, the three data sets were compared for consistency before the three results were averaged for final data reduction. Other pertinent information such as inlet and outlet temperatures of each heat exchanger, volumetric flow rates of each loop, steam outlet quality of the condensing channel, and condensing channel inlet pressure were also displayed on the screen to allow the operator to determine the validity of a given test. The final results, consisting of 30 data samples averaged for each measured variable, were stored in the computer for future processing as discussed below.

3.1. Inlet quality

The conservation of energy for the test section may be written as

$$q_s = q_c + q_{env}, \tag{1}$$

where q_{env} is the heat transfer rate to the environment, q_c is the heat transfer rate to the coolant, and q_s is the heat transfer rate from the condensing steam.

The coolant sensible heat was calculated from the change in enthalpies of the coolant channel as

$$q_c = \dot{m}_c(i_{cout} - i_{cin}), \tag{2}$$

where $\dot{m}_c$ is the mass flow rate of the coolant, and i_{cout} and i_{cin} are, respectively, the outlet and inlet enthalpies of the coolant.

Similarly, q_s is calculated from the change in enthalpies of the condensing channel as

$$q_s = \dot{m}_s\left(i_{sin} + x_{in}i_{fg} - i_{sout}\right), \tag{3}$$

where $\dot{m}_s$ is the mass flow rate of the steam in the condensing channel, i_{sin} is the inlet enthalpy of saturated liquid, x_{in} is the inlet quality of the steam, i_{fg} is the latent heat of vaporization, and i_{sout} is the outlet enthalpy of the condensate. In Eq. (3), it is assumed that when the steam reached the condensing channel in the test section, it was in the quality region and exited as subcooled liquid. The inlet quality can be found by substituting Eqs. (2) and (3) into Eq. (1):

$$x_{in} = \frac{\dot{m}_c(i_{cout} - i_{cin}) + q_{env} - \dot{m}_s(i_{sin} - i_{sout})}{\dot{m}_s i_{fg}}. \tag{4}$$

3.2. Local condensing heat transfer coefficients

In order to obtain local heat transfer coefficient results, Eq. (1) was applied incrementally along the test section:

$$\Delta q_s(z) = \Delta q_c(z) + \Delta q_{env}(z), \tag{5}$$

where $\Delta q_{env}(z)$ is the local heat transfer rate to the environment, and the local sensible heat gain of the coolant $\Delta q_c(z)$ was calculated from the change in local enthalpies of the coolant as

$$\Delta q_c(z) = \dot{m}_c[i_c(n) - i_c(n-1)], \tag{6}$$

where the index n refers to one of the test section segments.

Knowing the heat transferred in a test section segment along with the steam and wall temperatures allows the determination of the condensing heat transfer coefficient from Newton's law of cooling:

$$h(z) = \frac{\Delta q_s(z)}{\Delta A_s[T_s(z) - T_w(z)]} = \frac{\Delta q_c(z) + \Delta q_{env}(z)}{\Delta A_s[T_s(z) - T_w(z)]}, \tag{7}$$

where ΔA_s is the heat transfer surface area of a particular test segment, and $T_s(z)$ and $T_w(z)$ are the steam and wall temperatures, respectively. (It should be noted that the heat transfer surface area used to define the condensing heat transfer coefficient was set to one half of the entire channel surface area because it represents the physical process of bottom-surface condensation, including a fin effect of the side walls of the channel.) The local condensing heat transfer coefficients were evaluated at axial locations that corresponded to the measurements of the wall temperatures. The condensing steam temperatures, at the axial locations where wall temperatures were measured, were calculated from the measured inlet steam temperature and the steam pressure along the test section:

$$T_s(z) = f(p_s(z)), \tag{8}$$

where $p_s(z)$ is the local steam pressure.

The steam pressure drop was small (less than 3.5 kPa) in all tests so that the steam pressure was approximated as linear along the test section:

$$p_s(z) = p_{sin} - \frac{\Delta p}{L}z, \tag{9}$$

where p_{sin} is the inlet steam pressure, and Δp is the pressure drop across the test section.

3.3. Local qualities

Expanding Eq. (5) at a test section segment yields

$$\begin{aligned}\Delta q_s(z) &= \dot{m}_s[x(n-1) - x(n)]i_{fg}(z)\\ &= \Delta q_c(z) + \Delta q_{env}(z),\end{aligned} \tag{10}$$

where $i_{fg}(z)$, calculated from the local steam temperature, is the local latent heat of vaporization, and $x(n-1)$ and $x(n)$ are the inlet and outlet qualities of the steam at a particular test segment. From Eq. (10), the local quality can be expressed as

$$x(n) = x(n-1) - \frac{\Delta q_c(z) + \Delta q_{env}(z)}{\dot{m}_s i_{fg}(z)}. \tag{11}$$

Based on Eqs. (1)–(11), a data reduction code was written in spreadsheet format with Microsoft Excel. The data reduction requires information about the thermal and transport properties of water and MultiTherm as a function of pressure and temperature. Property data were based on the ASHRAE Handbook of Fundamentals [4] (for water) and on the MultiTherm IG-2 Physical Properties bulletin [5].

4. Heat loss calibration

The inlet quality, local condensing heat transfer coefficients and local qualities were calculated from

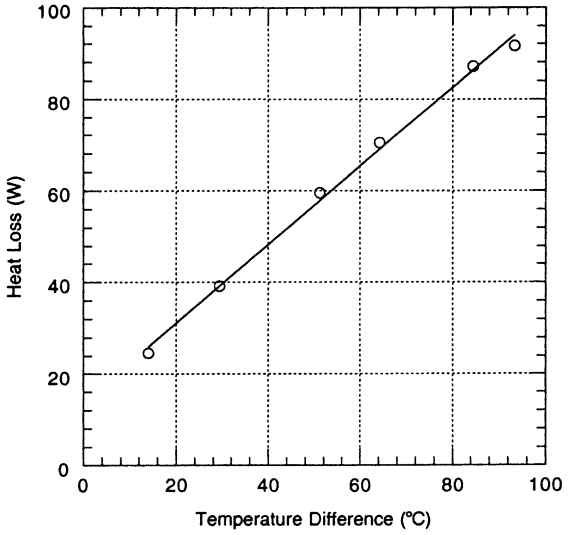

Fig. 3. Calibration of heat loss.

Eqs. (4), (7), (11), respectively, all of which involve the environmental heat loss. Because of the small test section size, low flow rates, and relatively high temperatures, the heat loss was not negligible, and its accurate characterization eliminated experimental error up to five percent. In order to measure test section heat loss, a series of single-phase heat transfer tests was performed at a condensing-channel fluid pressure of 965 kPa, a high flow rate, and various condensing-channel fluid inlet temperatures that ranged from ambient to 150 °C (the boiling temperature of water at 965 kPa is 178 °C). For each of the tests, heat loss was determined from a heat balance as

$$q_{\text{env}} = q_{\text{s}} - q_{\text{c}} = \dot{m}_{\text{s}}(i_{\text{sin}} - i_{\text{sout}}) - \dot{m}_{\text{c}}(i_{\text{cout}} - i_{\text{cin}}), \qquad (12)$$

where enthalpy i_{sin} refers to subcooled water at the inlet to the condensing channel.

The heat loss based on the single-phase heat transfer tests is plotted in Fig. 3 as a function of ΔT_{amb}. The linear relationship exhibited can be expressed as

$$q_{\text{env}} = (hA)\Delta T_{\text{amb}}. \qquad (13)$$

Eq. (13) was used in all condensing tests to account for heat loss to the environment. In all tests it was less than five percent of the heat transferred.

5. Experimental results and discussion

To investigate the effect of mass flux, pressure, and quality on the characteristics of internal one-sided condensing heat transfer, these parameters were varied independently in the test series. In each test, local values of the condensing heat transfer coefficient and quality were determined at multiple measurement points along the test section. The ranges of all of the experimental parameters are listed in Table 1. The parameter ranges of mass flux, pressure, and quality are also shown graphically with experimental Nusselt numbers in Figs. 4–6, respectively; they are discussed individually below.

Table 1
Value/range of experimental parameters

Parameter	Value/range
Flow channel	Rectangular channel
Flow direction	Horizontal
Hydraulic diameter D_{h} (mm)	10.8
Steam temperature T_{s} (°C)	115–160
Quality x (%)	10–80
Heat flux q''_{s} (W/m^2)	11 600–201 000
Mass flux G (kg/m^2 s)	20–50
Pressure p (kPa)	170–620
Reynolds number of liquid Re_{L}	910–2970
Prandtl number of liquid Pr_{L}	1.09–1.52

Uncertainties for experimental results were determined by using the method of sequential perturbation, as outlined by Moffat [6] for single-sample data. Uncertainties in each of the independent variables used to calculate the heat transfer coefficient were estimated on the basis of calibration and examination of system/sensor interaction errors. The resulting experimental uncertainties were less than seven percent for the condensing heat transfer coefficients in all tests of this study.

5.1. Mass flux impact

Local Nusselt numbers are plotted in Fig. 4 as a function of mass flux. The scatter in the plotted data is

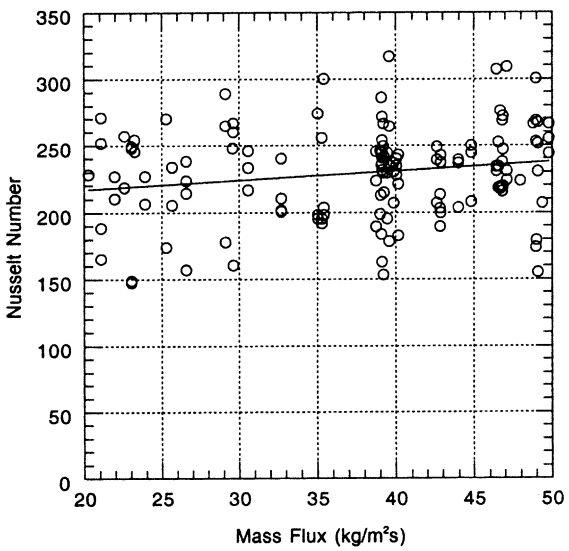

Fig. 4. Local Nusselt number as function of mass flux.

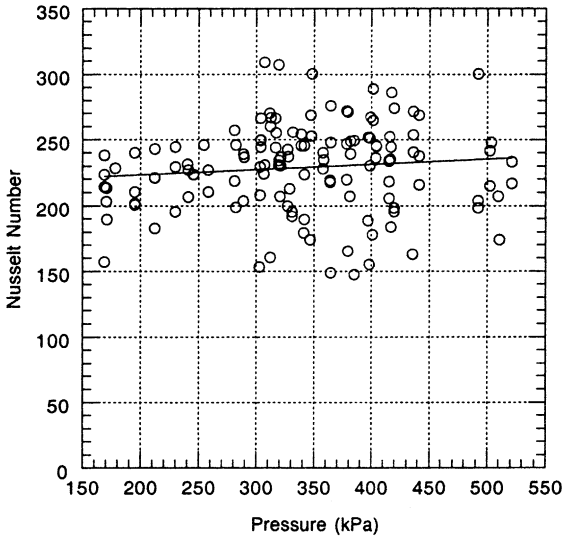

Fig. 5. Local Nusselt number as function of pressure.

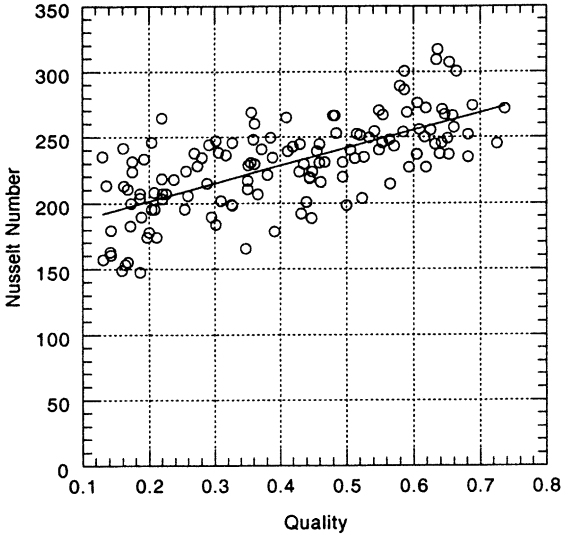

Fig. 6. Local Nusselt number as function of quality.

due in part to the influence of the other parameters (quality and pressure) that varied among these tests. However, a modest influence of mass flux is observed in Fig. 4, with the Nusselt number increasing very slightly with mass flux. This result is consistent with the relatively low mass flux range (< 50 kg/m^2 s) of the present data. This general trend in heat transfer coefficients in tubes has been reported by several investigators, e.g. [7]. At very low mass fluxes, the effect of mass flux on heat transfer coefficient has been observed to be essentially negligible [3,8,9].

5.2. Pressure impact

Local Nusselt numbers are plotted in Fig. 5 as a function of steam pressure. The pressure range of the present experiments is modest (170–620 kPa) and any trends attributable to pressure and fluid properties do not stand out in this plot. The effect of properties was considered in the correlation of the data, and good results were obtained.

5.3. Quality impact

Local Nusselt numbers are shown in Fig. 6 as a function of quality. The Nusselt numbers are seen to increase with increasing quality, and part of the data scatter in Fig. 6 is attributable to other parameters, such as mass flux and pressure, which are not controlled on this plot. In the current experiments, much of the condensate resides at the condensing surface, and the liquid film thickness at the surface increases as quality decreases. This situation is enhanced by the application of this study with one-sided condensing at the bottom surface of the channel with gravitational forces important at low mass fluxes. This quality trend is consistent over the entire range of the data. Although the liquid film thickness is low over this quality range (calculated from the thin film approach discussed subsequently as 0.05 mm $\pm$ 20% over the experimental quality range of 0.74–0.13), it decreased by over 40% from the highest to the lowest quality. This change is appreciable from the standpoint of the heat transfer coefficient.

5.4. Correlation of data

In the present study, condensing heat transfer occurred inside a rectangular channel with three insulated walls, at low mass fluxes (< 50 kg/m^2 s). No predictive equations for local heat transfer coefficient were found in the engineering literature appropriate for all of these conditions. To develop a correlation equation for predicting the data of this study, three approaches were followed. These three approaches were based on the work of Shah [10], Lu and Suryanarayana [3], and Akers and Rosson [9].

(a) *Shah correlation approach*. To put the heat transfer results into perspective, the Shah correlation, which is a widely cited correlation of the two-phase multiplier type, was selected for comparison with the experimental data. The Shah correlation is given as

$$Nu = 0.023 Re_{\mathrm{L}}^{0.8} Pr_{\mathrm{L}}^{0.4} \left[(1-x)^{0.8} + \frac{3.8 x^{0.76} (1-x)^{0.04}}{P_{\mathrm{r}}^{0.38}} \right], \tag{14}$$

where Nu is the Nusselt number, Re_{L} is the Reynolds number for all mass flowing as a liquid, Pr_{L} is the Prandtl

number of liquid, x is the quality, and p_r is the reduced pressure. The bracketed term properly approaches unity as x approaches 0, reducing to a single-phase liquid Nusselt number.

Fig. 7 shows the experimental local Nusselt numbers from this study and the values predicted by the Shah correlation. It is evident that the Shah correlation underpredicts the data, but, the scatter is reasonable. The work of Shah [10] covers a broad range of parameters, including the mass flux range and channel size of the present experiments. However, it does not include one-sided condensation nor a rectangular channel. Consequently, Eq. (14) was modified in an attempt to better predict the data.

Shah's condensing correlation equation is seen as a quality function correction to a single-phase, turbulent heat transfer correlation. It was observed that Eq. (14) underpredicted the present data over the entire quality range. Thus, in modifying Eq. (14) to better predict the current data, only the quality correction term was changed. Changes were made in ways that, like Eq. (14), reduce to single-phase heat transfer as quality goes to zero. The result is the modified correlation

$$Nu = 0.023\,Re_L^{0.8}\,Pr_L^{0.4}\left[(1-x)^{0.8} + \frac{14.1x^{0.5}(1-x)^{0.3}}{p_r^{0.25}}\right]. \tag{15}$$

Fig. 8 shows the experimental local Nusselt numbers with values predicted by Eq. (15). The predictions of Eq. (15) with the present experimental data are much improved over those predicted by Eq. (14) with most of the predicted data within 30%.

(b) *Thin-film correlation approach*. In a second approach to correlate present experimental data, the results of Lu and Suryanarayana [3] were used. In their investigations, Refrigerant R-113 and Fluorinert Compound FC-72 were condensed in a relatively large rectangular channel (40 mm wide by 25 mm high) that was cooled from the bottom only. Following the work of others, it was assumed that, for stratified flow, the heat transfer resistance was dominated by conduction across the thin condensate film. In the form of the local Nusselt number, this dominance is expressed as

$$Nu = \frac{D_h}{\delta}, \tag{16}$$

where the characteristic length D_h is the hydraulic diameter determined from the actual heat transfer surface area (for bottom surface condensation with side-wall fin effect) as

$$D_h = \frac{4W_sH_s}{W_s + H_s} \tag{17}$$

and δ is the condensate film thickness. In general, the condensate film thickness is a function of experimental parameters such as pressure, mass flux, and quality. As discussed previously, the condensing heat transfer coefficient is almost independent of pressure and mass flux in the present study, so the condensate film thickness was assumed to be a function of quality only in the present case. Following the approach of Lu and Suryanarayana [3], the condensate film thickness was assumed to follow a power law function

$$\delta = cx^{-\alpha}, \tag{18}$$

where c and α are constants determined from experimental data. Substituting Eq. (18) into Eq. (16) and optimizing the constants yields

$$Nu = 281.8x^{0.216}. \tag{19}$$

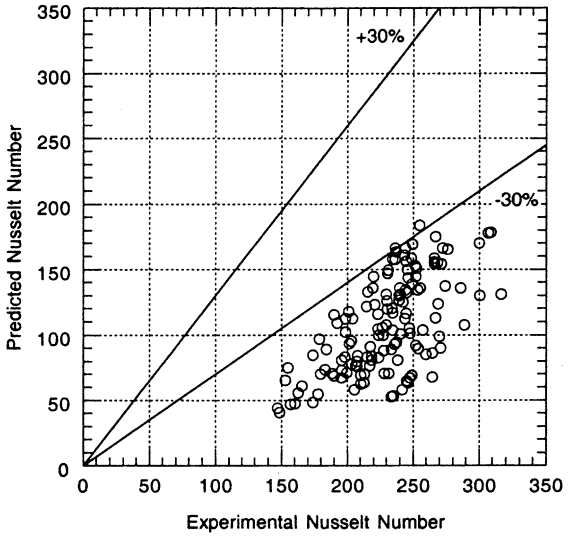

Fig. 7. Nusselt number predictions of Shah equation.

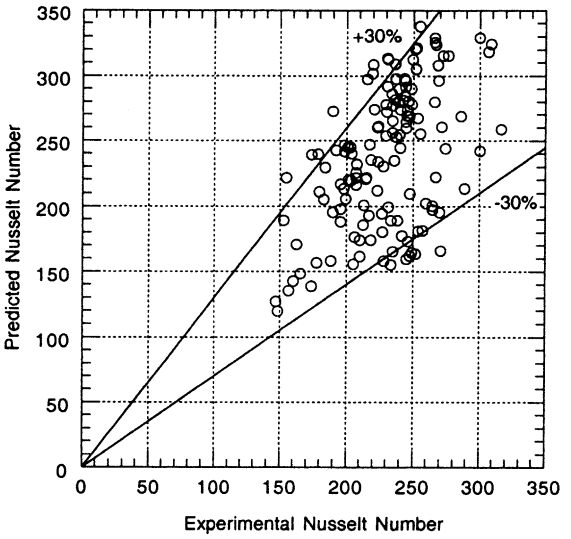

Fig. 8. Nusselt number predictions of modified Shah equation.

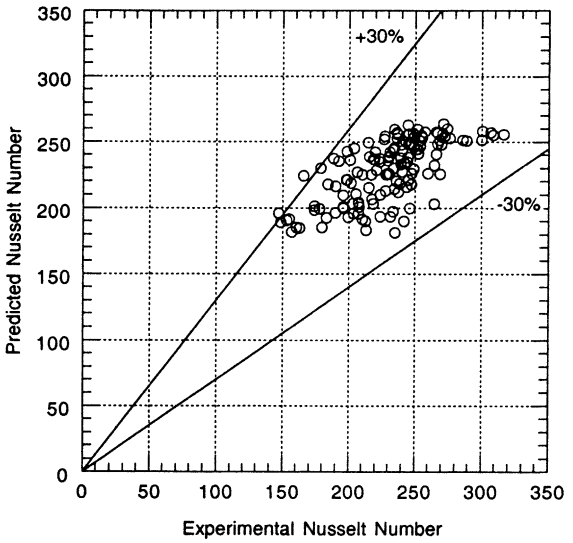

Fig. 9. Nusselt number predictions of thin-film equation.

Fig. 9 shows the experimental local Nusselt numbers and those predicted by Eq. (19). Eq. (19) predicts the experimental data quite well. Eq. (18) was then used to calculate liquid film thickness (as discussed previously with respect to data trends) predicting values in the range of 0.041–0.059 mm. Correspondingly, the liquid film velocity increased as the film thicken with reduced quality to a maximum of 0.24 m/s in the present experiments. The vapor velocity also increased with decreasing quality although the velocity slip ratio was highest at high qualities ranging from a slip of 1.18 to 17.2 in the present experiments. Although the large channel of Lu and Suryanarayana [3] was reported to have produced stratified flow, and the small channels of this study tend to produce slug flows [11], the liquid film domination of the heat transfer is relevant in both two-phase flow regimes as substantiated by the good predictions shown in Fig. 9.

(c) *Akers and Rosson correlation approach*. Based on the experimental data for methanol and Freon-12, Akers and Rosson [9] proposed the following correlation for condensing heat transfer inside horizontal tubes (when $DG_V/\mu_L < 5000$):

$$Nu = \begin{cases} 13.8\,Pr_L^{1/3}\left(\frac{i_{fg}}{C_{pL}\Delta T}\right)^{1/6}\left[\frac{DG_V}{\mu_L}\left(\frac{\rho_L}{\rho_V}\right)^{0.5}\right]^{0.2}, \\ \quad 1000 < \frac{DG_V}{\mu_L}\left(\frac{\rho_L}{\rho_V}\right)^{0.5} < 20000, \\ 0.1\,Pr_L^{1/3}\left(\frac{i_{fg}}{C_{pL}\Delta T}\right)^{1/6}\left[\frac{DG_V}{\mu_L}\left(\frac{\rho_L}{\rho_V}\right)^{0.5}\right]^{2/3}, \\ \quad 20000 < \frac{DG_V}{\mu_L}\left(\frac{\rho_L}{\rho_V}\right)^{0.5} < 100000, \end{cases} \quad (20)$$

where C_{pL} is the specific heat of liquid, ΔT is the temperature difference between saturated steam and the condensing surface, D is the tube diameter, C_V is the vapor mass flux based on the total cross section of the tube, μ_L is the liquid viscosity, ρ_L is the liquid density, and ρ_V is the vapor density. Eq. (20) describes the system in terms of the dynamic effects of the vapor on the liquid film $((DG_V/\mu_L)(\rho_L/\rho_V)^{0.5})$, the thermal properties of the liquid film (Pr_L), and the thermal potential $(i_{fg}/C_{pL}\Delta T)$.

Fig. 10 shows the experimental local Nusselt numbers together with values predicted by Eq. (20) where diameter was replaced with hydraulic diameter, as given in Eq. (17). It can be seen that although the Akers and Rosson correlation underpredicts the present experimental data slightly, the predicted errors are reasonable with respect to most of the data. It should be noted that this correlation is not as easily applied as Eqs. (15) and (19) because the wall temperature appears explicitly. However, Eq. (20) has been recommended by ASHRAE for many years [4], and the general agreement with the present data is gratifying.

The Akers and Rosson correlation differentiates between regimes of low and high values of a modified vapor Reynolds number based on vapor mass flux. In contrast, the data of the present study were seen to be rather insensitive to total mass flux, and the good predictions of Fig. 10 come from an insensitivity of Eq. (20) to mass flux in the low Reynolds number range. Sixty three percent of the present data fell into this low range where the vapor mass flux (as predicted from the thin film model) varied by only ±14%. (At the same time, the liquid film Reynolds number varied by ±99%. The liquid film approach to data correlation was essentially based on this parameter which showed a high degree of data sensitivity, and it was based exclusively on the quality

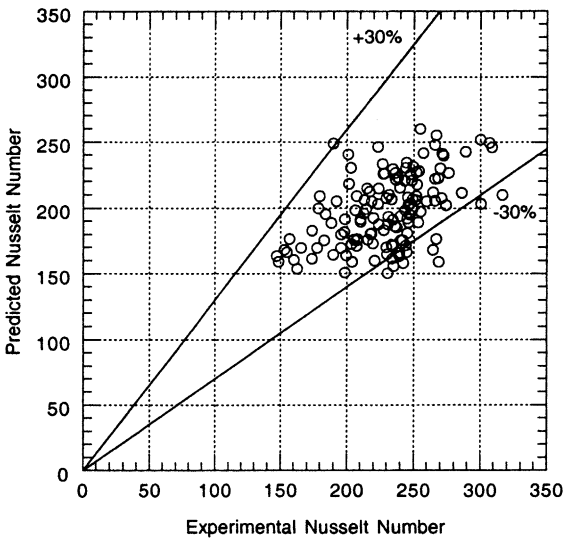

Fig. 10. Nusselt number predictions of Akers and Rosson equation.

which was the only parameter shown experimentally to significantly affect the heat transfer coefficient.)

6. Conclusions

To investigate the characteristics of condensing heat transfer inside of a small horizontal rectangular channel with the bottom surface cooled, experimental studies were undertaken in a specially designed condensing heat transfer apparatus. The following conclusions are drawn from this study at low mass flux.

The experimental results show that mass flux and pressure have relatively small effects on the Nusselt number. These results are mainly attributable to the low mass fluxes (< 50 kg/m^2 s) and the limited pressure range (170–620 kPa) of the present study. However, the Nusselt number was seen to increase with quality.

Because the Shah correlation [10] underpredicted the experimental data, it was modified to better predict experimental Nusselt numbers. The modified correlation retains the property effects of the Shah correlation and the reduction to the liquid case as quality goes to zero. The modification was accomplished through the quality effect consistent with data trends. Although the modified Shah equation predicted the present data reasonably well, it has an inherent dependence on mass flux that was not seen in the data of the present experiments with one-sided condensation at low mass flux.

The long-standing condensing heat transfer correlation of Akers and Rosson [9] predicted the present data reasonably well. However, like the Shah correlation, a mass flux dependence is inherent in the correlation that was not found in the data. The reasonable agreement between data and prediction was attributed to the relatively weak mass flux dependence of the correlation at low vapor Reynolds numbers.

Considering the three approaches to correlating the data presented, the adaptation of the liquid film domination approach of Lu and Suryanarayana [3] was the only one that omitted a mass flux effect consistent with the present data. In the present study, a thin-film dominant heat transfer correlation, based on the work of Lu and Suryanarayana [3], was developed. Although all three approaches to data prediction eventually predicted the present data reasonably well, the thin film approach was most consistent with the observed parameter trends. It is the recommended condensing heat transfer correlation for the data range of this investigation.

The present study was driven by application to steam drum dryers. The high rates of heat transfer found in the small, one-sided condensing channel of this study constitute a positive indication for the application of small channel condensation to such dryers.

Acknowledgements

This work was supported by the US Department of Energy, Office of Energy Efficiency and Renewable Energy, Office of Industrial Technologies, under Contract W-31-109-Eng-38. The authors wish to thank Valri Robinson and Ingrid Watson of the US DOE for support of this work. We thank Roger K. Smith for his contributions in fabricating the test apparatus, fabricating and instrumenting the test channel, and calibrating the instrumentation. We also acknowledge Nana D.K. Barde, William D. Vallance, and Carl W. Stewart of the Eastern Pulp and Paper Corporation for valuable discussions.

References

[1] M.K. Dobson, J.C. Chato, Condensation in smooth horizontal tubes, ASME J. Heat Transfer 120 (1) (1998) 193–213.
[2] S.U.S. Choi, W. Yu, D.M. France, M.W. Wambsganss, A novel multiport cylinder dryer, TAPPI J. 84 (2) (2001) 47.
[3] Q. Lu, N.V. Suryanarayana, Condensation of a vapor flowing inside a horizontal rectangular duct, ASME J. Heat Transfer 117 (2) (1995) 418–424.
[4] ASHRAE Handbook of Fundamentals, ASHRAE, Atlanta, GA, 1993.
[5] MultiTherm IG-2 Physical Properties: Bulletin MIG94, MultiTherm Corporation, Colwyn, PA, 1994.
[6] R.J. Moffat, Describing the uncertainties in experimental results, Exp. Thermal Fluid Sci. 1 (1) (1988) 3–17.
[7] N.Z. Azer, L.V. Abis, T.B. Swearingen, Local heat transfer coefficients during forced convection condensation inside horizontal tubes, ASHRAE Trans. 77 (1) (1971) 182–201.
[8] W.W. Akers, H.A. Dean, O. Crosser, Condensing heat transfer within horizontal tubes, Chem. Eng. Prog. Symp. Ser. 55 (29) (1959) 89–90.
[9] W.W. Akers, H.F. Rosson, Condensation inside a horizontal tube, Chem. Eng. Prog. Symp. Ser. 56 (30) (1960) 145–149.
[10] M.M. Shah, A general correlation for heat transfer during film condensation inside pipes, Int. J. Heat Mass Transfer 22 (4) (1979) 547–556.
[11] M.W. Wambsganss, J.A. Jendrzejczyk, D.M. France, Two-phase flow patterns and transitions in a small, horizontal, rectangular channel, Int. J. Multiphase Flow 17 (3) (1991) 327–342.